Supplemental Materials

Supplemental Methods

I. Outcomes Study Methods

Outcomes Study: Adjudication of CVD Events

Methodology employed for event adjudication in this cohort was previously described[1]. The definition of CVD is based on D'Agostino et al [2]. Briefly, CVD was defined as coronary death, myocardial infarction, coronary insufficiency, angina, ischemic stroke, hemorrhagic stroke, transient ischemic attack, peripheral artery disease, revascularization, or heart failure. Patients were categorized as having an acute coronary syndrome (ACS:ST-elevation MI or non-ST elevation MI or unstable angina) or new-onset stable angina based on the nature and duration of chest pain, medical history, and available diagnostics such as ECG and/or biomarkers, and as supported by findings on coronary arteriography.[3] Transient ischemic attack (TIA) was defined as the presence of focal neurological symptoms or signs lasting < 24 hours without signs of acute infarction on imaging[4] vs. ischemic stroke, characterized by focal neurologic symptoms in the distribution of symptomatic carotid artery lasting >24 and supported by findings on imaging such as CT.[5] 3) Peripheral arterial disease (PAD) was based on signs and symptoms (such as intermittent claudication, rest pain, ulcers, or gangrene) and non-invasive evaluation based on hemodynamic measures.[6] 4) Heart failure was defined based on signs and symptoms(such as dyspnea or fatigue or edema), medical history and diagnostics (such as ECG, chest radiograph, or two-dimensional echocardiography with Doppler).[7] 5) CVD death was defined as sudden death due to cardiovascular causes.

Outcomes Study: Measurement of regional brain ^{18}F-FDG uptake

Brain image analysis was performed by a radiologist (AI) blinded to all clinical data, using a workstation that enables multi-modal standard image fusion (Leonardo–TrueD, Siemens Solutions). After fusion of PET and CT datasets, the amygdala was localized on the CT images

using anatomic landmarks (see below for additional details). The amygdala is part of the limbic system located dorso-medially in the temporal lobe, forming the ventral superior, and medial walls of the inferior horn of the lateral ventricle. As such the lateral ventricles were used to define the anterior aspect, the anterior boundary was drawn when the inferior-most section of the lateral ventricles became flattened by the thalamus. The posterior boundary was defined by the crux of fornix and was always anterior to the basilar artery. The internal capsule was used as a guide for the lateral and inferior boundaries [8].

^{18}F-FDG uptake in amygdala was determined by placing a circular region of interest (ROI) in the defined structure bilaterally, and mean and maximum tracer accumulation were recorded as standardized uptake value (SUV) for each ROI. From this, amygdalar SUV was recorded for the left and right amygdala. Amygdalar activity was corrected for brain background activity, using cerebral (temporal lobe) and cerebellar (whole cerebellum) for separate background corrections [9]. The primary analysis for the study was the average of the maximum right and left amygdalar SUVs divided by the cerebral background (average max bilateral amygdala$_c$). Secondary endpoints were: average of the mean right and left amygdalar SUVs divided by the cerebral background (average average bilateral amygdala$_c$), and highest of the maximum right and left amygdala SUVs divided by the cerebral background (max max bilateral amygdala$_c$). Additional (exploratory) endpoints were also assessed, using the right or left amygdalar values alone, and/or correcting for cerebellar background activity.

Outcomes Study: Image analysis

Brain image analysis was performed by a radiologist (AI) blinded to all clinical data. Analysis of attenuation-corrected, PET and CT images were analyzed using a workstation that enables multi-modal standard image fusion (Leonardo–TrueD, Siemens Solutions, Malvern,

Pennsylvania, USA). After automated fusion of the PET and CT datasets, the amygdala was first localized on the CT images using anatomic landmarks. The amygdala is part of the limbic system located dorso-medially in the temporal lobe, forming the ventral superior, and medial walls of the inferior horn of the lateral ventricle. As such the lateral ventricles were used to define the anterior aspect, the anterior boundary was drawn when the inferior-most section of the lateral ventricles became flattened by the thalamus. The posterior boundary was defined by the crux of fornix and was always anterior to the basilar artery. The internal capsule was used as a guide for the lateral and inferior boundaries [8].

^{18}F-FDG uptake in amygdala was determined by placing a circular region of interest (ROI) in the defined structure bilaterally, and mean and maximum tracer accumulation were recorded as standardized uptake value (SUV) for each ROI. From this, amygdalar SUV was recorded for the left and right amygdala. Amygdalar activity was corrected for brain background activity, using cerebral (temporal lobe) and cerebellar (whole cerebellum) for separate background corrections [9]. The primary analysis for the study was the average of the maximum right and left amygdalar SUVs divided by the cerebral background (average_max bilateral amygdala$_c$). Secondary endpoints were: average of the mean right and left amygdalar SUVs divided by the cerebral background (average_average bilateral amygdala$_c$), and highest of the maximum right and left amygdalar SUVs divided by the cerebral background (max_max bilateral amygdala$_c$). Additional (exploratory) endpoints were also assess, using, the right or left amygdalar values alone, and/or correcting for cerebellar background activity.

Outcomes Study: Measurement of Hematopoietic Activity and Arterial Inflammation

These image analyses were performed by two investigators blinded to clinical data. Bone marrow and splenic activities were measured according to previously validated methods[10]. Bone marrow ^{18}F-FDG uptake was determined by placing ROIs in axial sections of individual

vertebrae from T1 to L5. The maximum SUV was recorded for each vertebra, and bone marrow activity was calculated as the average of the registered SUVmax of all measured vertebrae. Splenic ^{18}F-FDG uptake was determined by placing a ROI in each of axial, sagittal, and coronal sections. The SUVmax was recorded for each section, and splenic activity was calculated as the average of the three registered SUVmax values.

Arterial inflammation was assessed according to previously validated methods [10,11]. For the aortic wall, ^{18}F-FDG uptake was determined by placing circular ROIs in the axial sections around the vessel wall every 3 mm starting 1 cm above the aortic valve annulus and continuing to the bottom of the aortic arch. Background (venous blood) activity was measured in the lumen of the superior vena cava (SVC). Arterial target-to-background ratio (TBR) was calculated as aortic wall SUVmax values divided by blood background activity in SVC. Control extracranial tissue activity was measured as the mean SUV within subcutaneous adipose tissue, measured at the level of the umbilicus

Outcomes Study: Coronary calcium score assessment

Methodology employed for coronary calcium assessment in this cohort was previously described[1]. CAC score was quantitatively assessed (using pre-specified Hounsfield Unit range of >130 HU in ≥3 contiguous voxels) utilizing a dedicated workstation (TeraRecon AquariusWS, Version 3.7.0.8). Evaluation of CAC was performed using standardized methods[12] while blinded to clinical information and PET data by a separate group of investigators from those who performed the PET/CT analyses. The CAC scores measured on non-gated CT images obtained from a hybrid PET-CT scanner have been shown to be comparable to those obtained on a dedicated CT scanner [13].

Outcomes Study: Imaging Adipose Tissue Volume

Methodology employed for adipose tissue assessment in this cohort was previously described[1]. Fat volumes were measured by an investigator who was blinded to the clinical data as previously described using CT scans, with excellent inter- and intra-reader reproducibility (intra-class correlation coefficient=0.99).[14] Briefly, VAT volumes were measured using a dedicated offline workstation (Siemens Healthcare, Forchheim, Germany). Adipose tissue was identified using a threshold between -195 and -45 Hounsfield units (HU). The abdominal muscular wall was used as a boundary to separate VAT and subcutaneous adipose tissue (SAT). The volume was measured across all axial slices and was expressed as cm^3.

Outcomes Study: Statistical analysis

Statistical analyses were performed using SPSS (IBM Corp, Version 23). Continuous variables are listed as mean (±standard deviation (SD)), or when not normally distributed, as median (25^{th}-75^{th} percentile (P25-P75)). Univariate associations were evaluated using Pearson product-moment correlation and Spearman correlations coefficients for normally and non-normally distributed variable, respectively. After verifying the proportional hazard assumption for each variable used, Cox proportional hazards models were used, with or without the addition of potential confounders as covariates to calculate hazard ratios (HRs) and 95% confidence intervals. Covariates that were evaluated included age, gender, Framingham Risk Score, the existence of pre-existing atherosclerotic disease (as Coronary Artery Calcium), history of depression or anxiety, and antidepressant medications. When more than 3 co-variates were entered into a Cox model at one time, the cofactors were entered in a stepwise (backward) conditional manner. Time between imaging and date of event or last follow-up was entered into the Cox models. Furthermore, several subgroup analyses were performed to evaluate the relationship between amygdalar activity and CVD. Those subgroups included: A) individuals with or without pre-clinical evidence of atherosclerosis at baseline (as coronary atherosclerotic

calcification) , B) in individuals with or without a higher burden of coronary atherosclerotic risk factors, and C) in individuals with or without a prior history of cancer

Additionally, Kaplan-Meier estimates of CVD event-free survival was assessed (log rank tests) and survival curves were generated, comparing clinical events in those with high-vs low-amygdalar activity. In order to identify groups with high-vs lower- amygdalar activity, Receiver-Operator Curve (ROC) analysis was employed to delineate the amygdalar imaging values that have the highest accuracy to identify future events**.**

Missing data were dropped from relevant sub-analyses, imputation was not employed. Statistical significance was determined as two-tailed $p<0{\cdot}05$.

Mediation analysis was performed using the SPSS PROCESS macro, to test whether amygdalar activity exerts its effect on CVD via postulated mediators (bone marrow activity and arterial inflammation), either singularly or in series. The mediation analysis employed an ordinary least squares or logistic regression-based path framework to estimate direct and indirect effects and produced confidence intervals based upon 5,000 bias-corrected bootstrap samples.[15] We examined two hypothesized single mediator paths (PROCESS Model 4): a) amygdalar activity → bone marrow activity → arterial inflammation, and b) amygdalar activity → arterial inflammation → CVD event; as well as one hypothesized serial two-mediator path (PROCESS Model 6): c) amygdalar activity → bone marrow activity → arterial inflammation → CVD event. All analyses incorporated age, gender, and baseline coronary artery calcification (as a control for pre-existing atherosclerotic disease burden) as covariates.

II. Perceived Stress Study Methods

Perceived Stress Study Subject Selection and Perceived Stress Assessment

Study participants were recruited from physician referrals, media advertisement, and an academic outpatient psychiatrist clinic. Patients had chronic PTSD that was the primary presenting problem as assessed by a trained rater using the Structured Clinical Interview for DSM-IV (SCID-IV) and the Clinician-Administered PTSD Scale for DSM-IV (CAPS). Patients completed a battery of self-report measures that assessed variables that may correlate with PTSD symptom severity, including comorbid depressive and anxiety symptoms (MADRS, HAM-A) and a well-validated questionnaire Perceived Stress Scale (PSS-10)[16]. 13 subjects (ages: 29-61, 5F, 8M) were included in this analysis.

Perceived Stress Study: Imaging

Imaging of the head and neck was performed for evaluation of amygdalar and carotid arterial FDG uptake. Briefly, PET image acquisition was performed on a_MR/PET (3T) Siemens mMR (Siemens Healthcare, Erlangen, Germany). The 3T MR/PET is a fully integrated system, capable of simultaneous whole body PET and MRI scanning. Patients were asked to fast for at least 6 hours before injection of ~370mBq 18F-FDG. After injection subjects were instructed to rest in a room for about 30 minutes, to allow for tracer circulation and accumulation. Thereafter localizer scans were obtained then brain PET was acquired for 15 minutes, using one bed position covering the whole head. A T1 weighted Magnetization Prepared Rapid Acquisition Gradient Echo (MP RAGE) anatomical scan was also acquired simultaneously with brain PET acquisition. At 90 minutes after injection, carotid imaging was performed, (10 minutes per bed). Simultaneously with PET acquisition, black blood, 3D T2 weighted turbo spin echo (TSE) images were acquired. These images were used in the image analysis phase to identify the vasculature and draw regions of interest in the vessel wall. All PET data were acquired in 3D mode and were reconstructed after attenuation correction of the PET signal. The sequence used for attenuation correction in the

integrated PET/MRI system is a 2-point Dixon volume-interpolated breath-hold examination (VIBE). This sequence is preceded by scanning preparations that include shimming to optimize the homogeneity of the magnetic field (~40 s). The MRI data are then segmented to identify air, lung tissue, fatty tissue, and watery tissue as required for AC.

Perceived Stress Study: Image Analysis:

Image analysis for the Perceived Stress Study followed the methods of the Outcomes Study, with minor differences in the approach owing to the use of MR to derive structural information in the Perceived Stress Study (as opposed to the use of CT in the Outcomes Study). In brief, after reconstruction, PET images were transferred to an imaging workstation and analyzed using Osirix software (http://osirix-viewer.com). For the brain analysis, regions of interests (ROIs) in the amygdala were drawn on the anatomical MRI scans. For carotids, T2W images were reformatted in the axial plane. ROIs encompassing the whole vessel were traced on each axial slide from the carotid bifurcation downwards, and in the thoracic aorta. 5 ROIs were also traced on each side of the jugular vein and in the superior vena cava, to correct vessel wall uptake for blood activity and calculate target-to-background ratio (TBR). Both brain and vascular ROIs were transferred to the co-registered PET images to extract SUV parameters. Notably, the definitions for amygdalar endpoints followed those defined in the Outcomes Study.

III. Supplemental Results

Supplemental Table 1A. Correlation Coefficients for Amygdalar Activity vs Cardiac Risk Factors

Risk Factors	Amygdalar Measurement		
	maxmax amygdala$_c$	meanmean amygdala$_c$	meanmax amygdala$_c$
Age	0.116*	0.190†	0.123*
Male	-0.035	0.010	-0.022
Current Smoking	0.021	0.091	0.035
HTN	0.030	0.085	0.032
SBP	-0.024	0.060	-0.012
Family History of CAD	0.162*	0.163*	0.172*
History of Dyslipidemia	-0.059	-0.012	-0.063
DM	0.085	0.106	0.081
Total Chol	-0.016	-0.043	-0.016
LDL	-0.043	-0.063	-0.042
FRS	0.133	0.144	0.123

HTN = hypertension;
SBP = systolic blood pressure;
DM = diabetes mellitus;
Chol = cholesterol;
Trig, = triglycerides;
HDL = high density lipoprotein;
LDL = low density lipoprotein,
FRS = Framingham Risk Score.
*P<0.05 , † P<0.01 ,
Amygdalar activity was corrected for background (cerebral [c]) activity

Supplemental Table 1B. Meaan (+/- SD) amygdalar activity according to age and Family History of CAD

Endpoints	Amygdalar Measure	Family History of CAD		Age	
		FamHx +	FamHx -	≤median	>median
Primary Amygdalar Measurement	maxmax $amygdala_c$	1.04±0.24*	0.98±0.15*	1.00±0.15	1.02±0.20
Secondary Amygdalar Measurement	meanmean $amygdala_c$	0.84±0.19*	0.79±0.11*	0.95±0.13	0.98±0.17
Secondary Amygdalar Measurement	meanmax $amygdala_c$	1.00±0.22*	0.94±0.13*	0.78±0.10‡	0.82±0.14‡

*P<0.05 , † P<0.01 , ‡P≤0.001 (vs comparator group)
Amygdalar activity was corrected for background (cerebral [c] activity).

Supplemental Table 2: CVD Events

Subj.	Category	CVD	MACE	A-MACE	Notes
1	MI	x	x	x	1) STEMI, 100% RCA occlusion, 2) culprit coronary PCI 3) death associated with MI
2	PAD	x	x	x	1) New PAD requiring stenting for lower extremity ischemia/infection 2) non-cardiac death
3	MI	x	x	x	1) Silent IMI 2) 1 month later developed progressive CP: RCA stenosis 3) culprit coronary PCI
4	UA	x	x	x	1) UA; 2 vessel CAD including 100% LAD and 70% RCA stenoses
5	MI	x	x	x	1) NSTEMI, 99% First diagonal artery stenosis 2) culprit coronary PCI
6	CVA	x	x	x	1) thalamic CVA, and 2) UA with multi-vessel CAD requiring 3) CABG
7	MI	x	x	x	1) Anterior STEMI, 2) cardiac death
8	CVA	x	x	x	1) TIA associated w ipsilateral ICA stenosis
9	UA	x	x	x	1) UA associated with mid RCA stenosis 2) culprit PCI
10	MI	x	x	x	1) STEMI, with mid Left Circumflex stenosis 2) culprit coronary PCI
11	CVA	x	x	x	1) CVA and occluded L internal carotid artery and stenosis, 2) Non-cardiac death
12	UA	x	x	x	1) New exertional dyspnea associated with 70% left main stenosis, 2) culprit coronary PCI
13	MI	x	x	x	1) NSTEMI. Found to have severe Left main coronary artery disease, 2) CHF, systolic LV dysfunction
14	PAD	x	x	x	1) PAD by ABI and 2)severe, symptomatic L carotid arterial disease, 3) requiring CEA
15	MI	x	x	x	1) NSTEMI, found to have RCA and LCx disease, 2) underwent L carotid endarterectomy.
16	MI	x	x		1) NSTEMI : Chest pain and transient troponin elevation without significant occlusive coronary disease on coronary angiogram: ?embolism or spasm
17	CHF	x	x		1) new CHF. Found to have non-ischemic LV dysfunction
18	CVA	x	x		1) bilateral thalamic CVAs, no significant carotid disease
19	CVA	x	x		1) TIA (transient vision loss). Mild plaque in carotid ultrasound
20	CVA	x	x		1) Right occipital ischemic infarction thought due to hypertension
21	CP	x			1) Worsening exertional CP, improved with NTG. Angiogram: mild LAD disease
22	CP	x			1) recurrent chest pains radiating down arm. Mild CAD
Totals		22	20	15	39 Events (22 primary and 17 secondary) events

Supplemental Table 3 .Control Tissue Activity Does Not Associate with CVD Events

Adjustment		Hazard Ratio from Cox Models	HR for Control Tissue Activity (SUV) Measurement		
			Control *Cerebral* Tissue	Control *Cerebellar* Tissue	Control *Extra-cranial* Tissue
			Temporal Lobe	Cerebellum	SubQ Fat
No Co-Variates	Univariate	unstandardized	0.8 (0.6-1.1)	0.9 (0.7-1.2)	10.0 (0.0-7348)
Co-Variates	Age and Gender	unstandardized	1.0 (0.7-1.4)	1.0 (0.7-1.3)	0.4 (0.0-868)
	Framingham Risk Score	unstandardized	0.9 (0.7-1.3)	0.9 (0.7-1.2)	1.4 (0.0-2623)

SubQ= Subcutaneous
P=NS for all assessments
All HRs per unit activity.

Supplemental Table 4 Additional Adjustments for Clinical Variables

Multivariate Adjustments		HR (95% CI) for Amygdalar Measurements			
		Primary Measure	**Secondary Measure**	**Secondary Measure**	**Post-Hoc Measure**
		maxmax $Amygdala_c$	**meanmean $Amygdala_c$**	**meanmax $Amygdala_c$**	**mean L $Amygdala_{cbl}$**
Cox model analysis of amygdalar activity vs. CVD events after adjustments for clinical factors	Univariate	14.1‡ (4.0-50.0)	41.1‡ (8.7-194.5)	19.4‡ (4.7-79.9)	101.4‡ (12.5-822.4)
	Family History	8.0‡ (2.3-27.5)	15.0 (2.9-76.3)‡	9.3† (2.3-38.4)	34.7‡ (4.7-257.9)
	Diabetes	16.3 ‡ (4.3-61.3)	53.2 ‡ (10.4-273.0)	16.3 ‡ (4.3-61.3)	108.1 ‡ (12.5-930.7)
	Statins and dyslipidemia	67.8‡ (12.7-362.8)	29.1‡ (6.4-133.1)	19.8 ‡ (5.2-75.7)	158 ‡ (17.4-1435)
	Smoking	17.2 ‡ (4.6-64.0)	46.2‡ (9.0-236.2)	23.7‡ (5.4-103.4)	126.1‡ (14.4-1103.3)
	Prior cancer	25.3 ‡ (5.1-126.4)	14.9 ‡ (3.7-60.5)	11 ‡ (3.2-38.1)	47.5 ‡ (5.8-388.8)
	Prior chemo	35.6 ‡ (7.5-168.1)	18.2‡ (4.4-74.8)	13.2 ‡ (3.8-46.4)	76.2 ‡ (9.3-625.0)

*P<0.05 , † P<0.01 , ‡P≤0.001 Amygdalar activity was corrected for background (cerebral [c] or cerebellar [cbl] neural tissue activity). All HRs per unit activity.

Supplemental Table 5. Adjustment for other Imaging Measures of CVD Risk

	Hazard Ratio from Cox Model	HR (95% CI) for Amygdalar Measurements			
		Primary Measure	Secondary Measure	Secondary Measure	Post-Hoc Measure
		maxmax $Amygdala_c$	**meanmean $Amygdala_c$**	**meanmax $Amygdala_c$**	**mean L $Amygdala_{cbl}$**
Adjust for CAC Volume	unstandardized	10.7 ‡ (2.6-42.9)	31.7‡ (5.8-172.8)	14.3‡ (3.0-68.0)	55.5‡ (5.0-614.3)
Adjust for VAT Volume	unstandardized	8.7‡ (2.5-31.0)	16.7‡ (3.3-84.9)	11.8‡ (2.8-49.6)	22.2† (2.9-168.2)

*P<0.05 , † P<0.01 , ‡P≤0.001 Amygdalar activity was corrected for background (cerebral [c] or cerebellar [cbl] neural tissue activity). All HRs per unit activity.

Supplemental Table 6. Sensitivity analysis: Alternate measures of amygdalar activity vs. CVD

Amygdalar Measure	Hazard Ratio from Cox Model	HR (95% CI) for Univariate Analysis	HR (95% CI) for Multivariate Analyses	
			Age and gender adjustment	FRS Adjustment
mean Right $amygdala_c$	unstandardized	19.6‡ (4.8-79.2)	5.6* (1.2-25.4)	5.2* (1.3-21.4)
max Right $amygdala_c$	unstandardized	12.4‡ (3.5-41.9)	4.3* (1.2-16.2)	4.1* (1.2-13.9)
mean Left $amygdala_c$	unstandardized	81.3‡ (13.8-480.7)	27.7‡ (3.7-207.1)	15.4† (2.5-94.0)
max Left $amygdala_c$	unstandardized	25.1‡ (4.6-1356.0)	6.5* (1.2-36.1)	5.6* (1.1-28.2)
meanmean Bilat $amygdala_{cbl}$	unstandardized	57.8‡ (9.1-368.5)	23.1‡ (3.9-137.2)	16.5‡ (3.1-88.3)
meanmax Bilat $amygdala_{cbl}$	unstandardized	24.1‡ (4.0-144.3)	11.7† (2.4-57.1)	9.331† (2.0-43.6)
maxmax Bilat $amygdala_{cbl}$	unstandardized	17.6‡ (3.8-82.7)	9.6† (2.3-38.8)	7.746† (2.0-30.1)
mean Right $amygdala_{cbl}$	unstandardized	29.4‡ (5.4-160.9)	11.0 † (2.2-54.7)	9.5† (2.1-43.7)
max Right $amygdala_{cbl}$	unstandardized	15.6‡ (3.4-70.9)	8.0† (2.0-31.7)	6.6† (1.8-25.0)
mean Left $amygdala_{cbl}$	unstandardized	101.3‡ (12.5-822.4)	53.0 ‡ (7.4-379.8)	29.0‡ (4.6-183.7)
max Lleft $amygdala_{cbl}$	unstandardized	24.8† (3.0-206.6)	15.7† (2.5-100.2)	12.4† (2.0-78.2)

*P<0.05 , † P<0.01 , ‡P≤0.001 Amygdalar activity was corrected for background (cerebral [c] or cerebellar [cbl] neural tissue activity). All HRs per unit activity.

Supplemental Table 7. Correlations Between Hematopoietic Tissue Activity and Blood Cells

Blood Measurement	Spleen Activity (SUV)	Bone Marrow Activity (SUV)
	r Value	r Value
WBC (th/cmm)	0.12	0.196‡
Mono (th/cmm)	-0.03	0.04
Neutr (th/cmm)	0.10	0.169*
Lymph (th/cmm)	0.192‡	0.152*
Eos (th/cmm)	-0.05	0.00
Baso (th/cmm)	0.02	0.01
RBC (mil/cmm)	0.12	0.164*
Hct (%)	-0.04	0.03
Hgb (gm/dl)	-0.06	-0.02
Plat (th/cumm)	-0.01	0.146*
WBC:Hgb	0.133*	0.190‡
WBC:RBC	0.097	0.140*

*P<0.05 , † P<0.01 , ‡P≤0.001 for relationship between cellular assay and hematopoietic tissue SUV

Supplemental Table 8 Subject Characteristics for Perceived Stress Study

Characteristics	**Full Cohort** (n=13)
Age, yrs ; Median, (IQR)	48 (45.7-53.2)
Male; N, (%)	8 (61.5%)
Caucasian; N, (%)	1 (7.69%)
Current smoker ; N, (%)	4 (30.8%)
Hypertension; N, (%)	4 (30.8%)
Diabetes mellitus; N, (%)	2 (15.4%)
Hyperlipidemia; N, (%);	0 (0%)
Total cholesterol; Mean, (SD)	179.9 (25.0)
LDL; Mean, (SD)	106.7 (26.2)
BMI, kg/m2 ; Median, (IQR)	29.5 (27.2-30.8)
History of cancer; N, (%)	0 (0%)
History depression or anxiety; N, (%)	10 (76.9%)
Anti-depressant medication use; N, (%)	1 (7.69%)

LDL= Low Density Lipoproteins

BMI= Body Mass Index

Supplemental Figure 1. Survival curves for high-vs low amygdalar activity

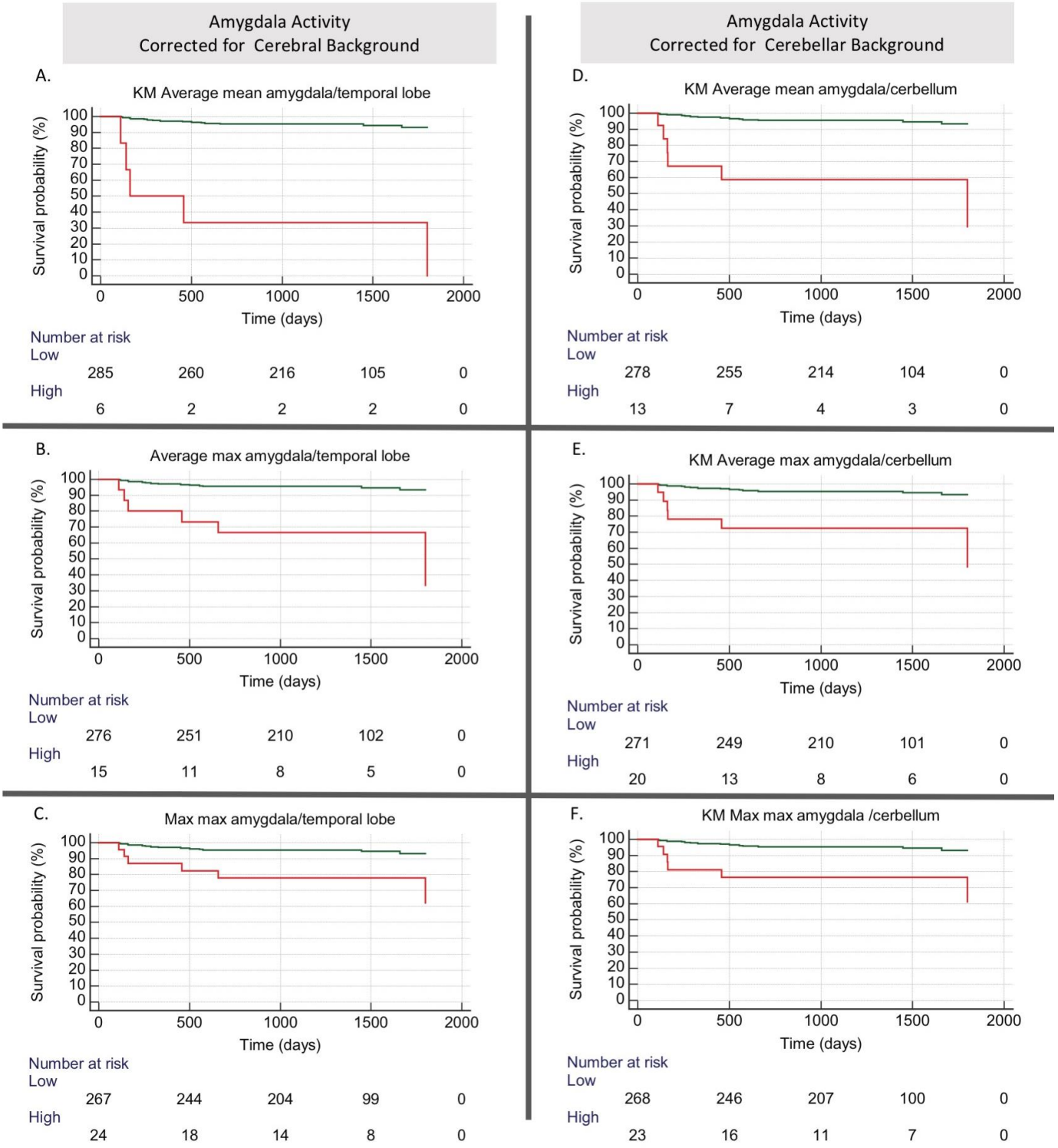

Values that define “high” vs “lower” activity for these curves were defined using ROC analyses.

Supplemental Fig 2: Amygdalar Activity vs Timing of Events

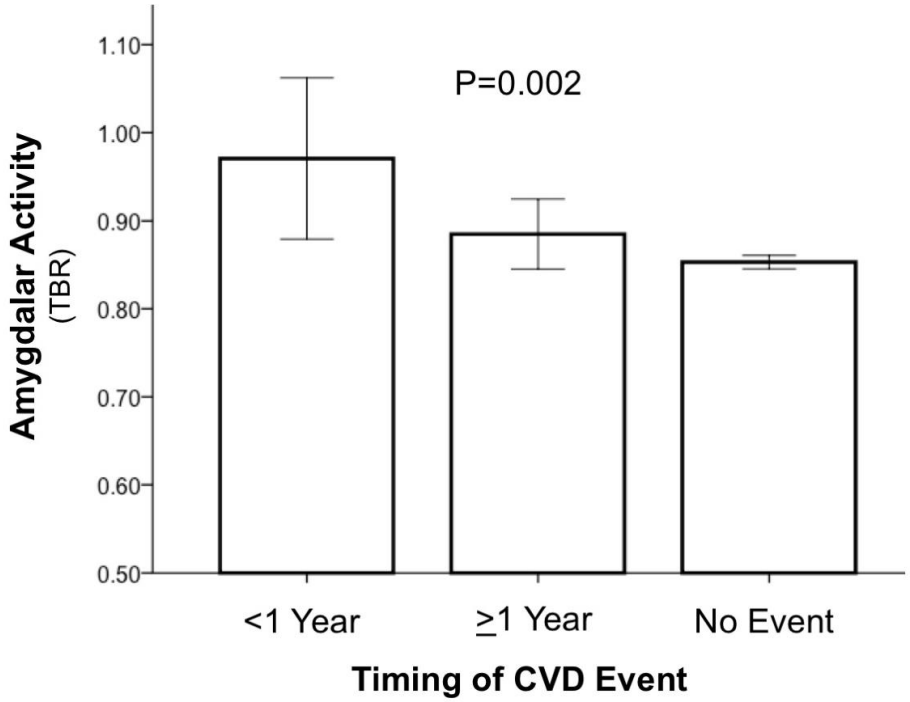

Error bars indicate +/-1 SD

Individuals were grouped according to the timing of the CVD event relative to index imaging. Individuals with early CVD events (within 1 year of imaging) had the highest baseline amygdalar activity, followed by individuals with later events, followed by individuals who did not experience a CVD event during the follow-up period.

Supplemental References

1. Figueroa AL, Abdelbaky A, Truong QA, et al. Measurement of Arterial Activity on Routine FDG PET/CT Images Improves Prediction of Risk of Future CV Events. *JACC Cardiovasc Imaging* 2013; **6**(12): 1250-9.
2. D'Agostino RB, Sr., Vasan RS, Pencina MJ, et al. General cardiovascular risk profile for use in primary care: the Framingham Heart Study. *Circulation* 2008; **117**(6): 743-53.
3. Anderson JL, Adams CD, Antman EM, et al. 2011 ACCF/AHA Focused Update Incorporated Into the ACC/AHA 2007 Guidelines for the Management of Patients With Unstable Angina/Non-ST-Elevation Myocardial Infarction: a report of the American College of Cardiology Foundation/American Heart Association Task Force on Practice Guidelines. *Circulation*; **123**(18): e426-579.
4. Furie KL, Kasner SE, Adams RJ, et al. Guidelines for the prevention of stroke in patients with stroke or transient ischemic attack: a guideline for healthcare professionals from the american heart association/american stroke association. *Stroke; a journal of cerebral circulation*; **42**(1): 227-76.
5. Mauriello A, Sangiorgi GM, Virmani R, et al. A pathobiologic link between risk factors profile and morphological markers of carotid instability. *Atherosclerosis*; **208**(2): 572-80.
6. Hiatt WR, Goldstone J, Smith SC, Jr., et al. Atherosclerotic Peripheral Vascular Disease Symposium II: nomenclature for vascular diseases. *Circulation* 2008; **118**(25): 2826-9.
7. Hunt SA, Abraham WT, Chin MH, et al. 2009 Focused update incorporated into the ACC/AHA 2005 Guidelines for the Diagnosis and Management of Heart Failure in Adults A Report of the American College of Cardiology Foundation/American Heart Association Task Force on Practice Guidelines Developed in Collaboration With the International Society for Heart and Lung Transplantation. *Journal of the American College of Cardiology* 2009; **53**(15): e1-e90.
8. Abercrombie HC, Schaefer SM, Larson CL, et al. Metabolic rate in the right amygdala predicts negative affect in depressed patients. *Neuroreport* 1998; **9**(14): 3301-7.
9. Britz-Cunningham SH, Millstine JW, Gerbaudo VH. Improved discrimination of benign and malignant lesions on FDG PET/CT, using comparative activity ratios to brain, basal ganglia, or cerebellum. *Clinical nuclear medicine* 2008; **33**(10): 681-7.
10. Emami H, Singh P, MacNabb M, et al. Splenic metabolic activity predicts risk of future cardiovascular events: demonstration of a cardiosplenic axis in humans. *JACC Cardiovasc Imaging* 2015; **8**(2): 121-30.
11. Subramanian S, Emami H, Vucic E, et al. High-dose atorvastatin reduces periodontal inflammation: a novel pleiotropic effect of statins. *J Am Coll Cardiol* 2013; **62**(25): 2382-91.
12. Blaha MJ, Budoff MJ, DeFilippis AP, et al. Associations between C-reactive protein, coronary artery calcium, and cardiovascular events: implications for the JUPITER population from MESA, a population-based cohort study. *Lancet* 2011; **378**(9792): 684-92.
13. Einstein AJ, Johnson LL, Bokhari S, et al. Agreement of visual estimation of coronary artery calcium from low-dose CT attenuation correction scans in hybrid PET/CT and SPECT/CT with standard Agatston score. *Journal of the American College of Cardiology* 2010; **56**(23): 1914-21.

14. Maurovich-Horvat P, Massaro J, Fox CS, Moselewski F, O'Donnell CJ, Hoffmann U. Comparison of anthropometric, area- and volume-based assessment of abdominal subcutaneous and visceral adipose tissue volumes using multi-detector computed tomography. *Int J Obes (Lond)* 2007; **31**(3): 500-6.
15. Hayes A. Introduction to Mediation, Moderation, and Conditional Process Analysis: A Regression-Based Approach. New York, NY: Guilford Press; 2013.
16. Cohen S, Kamarck T, Mermelstein R. A global measure of perceived stress. *Journal of health and social behavior* 1983; **24**(4): 385-96.